Electronic Supporting Information

R-phycoerythrin extraction and purification from fresh *Gracilaria* sp. using thermo-responsive systems

Filipa A. Vicente[a], Inês S. Cardoso[a], Margarida Martins[a], Cátia V. M. Gonçalves[b], Ana C. R. V. Dias[b], Pedro Domingues[c], João A. P. Coutinho[a], Sónia P. M. Ventura[a,*]

[a]CICECO, Departamento de Química, Universidade de Aveiro, 3810-193 Aveiro, Portugal

[b]CESAM - Centre for Environmental and Marine Studies, Department of Environment and Planning, University of Aveiro, 3810-193 Aveiro, Portugal

[c]Centro de Espectrometria de Massa, Departamento de Química & QOPNA, Departamento de Química, Universidade de Aveiro, 3810-193 Aveiro, Portugal

[*]Corresponding author

Campus Universitário de Santiago, University of Aveiro, Aveiro, Portugal

Tel: +351-234-370200; Fax: +351-234-370084; E-mail address: spventura@ua.pt

Table S1. Inputs for both scenarios considered: (i) AMTPS without SAIL in the first liquid-liquid extraction and (ii) AMTPS with SAIL. The amounts indicated were determined for 5 g of algae fresh cells.

Stages	Input	AMTPS without SAIL	AMTPS with SAIL
		kg (or kWh for electricity)	
Algae	Tap water	0.0450	0.0450
Biomass pre-treatment	Liquid nitrogen	0.0121	0.0121
	Electricity	8.12×10^{-3}	8.12×10^{-3}
Solid-liquid extraction	Distilled water	7.20×10^{-3}	7.20×10^{-3}
Extraction	Electricity	1.07	1.07
1st liquid-liquid extraction	Citric acid*	6.78×10^{-5}	6.76×10^{-5}
	Sodium phosphate*	4.68×10^{-4}	4.66×10^{-4}
	Distilled water	0.0200	0.0199
	Tergitol 15-S-7	2.50×10^{-3}	2.50×10^{-3}
	$[N_{1,1,12,(C7H7)}]Br$	-	7.50×10^{-5}
	Electricity	5.30	5.30
2nd liquid-liquid extraction	Tergitol 15-S-7	1.00×10^{-3}	1.00×10^{-3}
	$[N_{1,1,12,(C7H7)}]Br$	3.00×10^{-5}	3.00×10^{-5}
	Electricity	5.20	5.20

*McIlvaine buffer

Table S2. GHG emission factors and activity name taken from Ecoinvent version 3.4 used in the calculation of the carbon footprint.[23]

Input	**Reference Unit**	**Activity name**	**GHG emissions (kg CO_2eq/reference unit)**[a]
Tap water	kg	-	0.001
Distilled water	kg	-	0.311
Electricity	kWh	Market for electricity, low voltage, Portugal	0.413
Liquid nitrogen	kg	Nitrogen liquid, air separation, cryogenic, Europe	0.253
McIlvaine buffer	kg	Citric acid production, Europe	3.068
McIlvaine buffer	kg	Sodium phosphate production, Europe[b]	3.054
Tergitol 15-S-7	kg	Ethoxylated alcohol (AE11) production, palm oil, Europe	2.866
$[N_{1,1,12,(C7H7)}]Br$	kg	Chemical production, organic, Global[d]	1.955

[a] Global warming potentials for converting the mass of each GHG into mass of CO_2eq are those recommended by the Intergovernmental Panel on Climate Change (IPCC) [25] for a time horizon of 100 years.

[b] In the absence of data for the production of sodium hydrogen phosphate, this process was selected as more similar.

[c] In the absence of data for the production of $[N_{1,1,12,(C7H7)}]Br$, this process was selected as more similar.

Table S3. Proteomic analysis of the proteins present in the phycobiliproteins crude extract after a solid-liquid extraction from fresh *Gracilaria sp.*

Accession	Description	Coverage [%]	# Peptides	# PSMs	# Unique Peptides	# AAs	MW [kDa]	calc. pI	Score MS Amanda 2.0	Score Sequest HT	Biological Process	Abundance (%)
W8DWF3	R-phycoerythrin alpha subunit	47	12	1351	3	164	17.7	5.35	242393.1	2732.7	metabolic process; transport	44.20
Q7SIF9	R-phycoerythrin beta chain	29	6	598	3	177	18.6	5.31	84231.9	890.2	metabolic process; transport	15.15
A0A088AXT1	Ribulose bisphosphate carboxylase large chain	40	41	787	20	488	54.2	6.55	121979.6	556.6	metabolic process	9.81
A0A141SEN3	Phycocyanin alpha subunit	75	12	442	12	162	17.6	7.12	72639.5	663.0	metabolic process; transport	5.06
Q6B8S6	Allophycocyanin beta subunit	89	17	385	8	161	17.5	5.31	63156.8	684.5	metabolic process; transport	4.74
A0A141SEN2	Phycocyanin beta subunit	51	10	700	2	172	18.2	5.11	107200.3	1033.8	metabolic process; transport	4.59
A0A1C9CES5	Allophycocyanin alpha subunit	75	15	356	2	161	17.5	5.01	46998.2	469.1	metabolic process; transport	3.99
A0A1P8D6I9	Ribulose-1,5-bisphosphate carboxylase/oxygenase small subunit	49	5	133	2	138	16.2	5.57	19103.2	245.8		3.79
P30724	Glyceraldehyde-3-phosphate dehydrogenase, chloroplastic	52	18	223	18	416	44.3	7.37	36490.0	369.8	metabolic process	1.76
A0A1C9CET6	ATP synthase subunit beta	39	15	255	2	475	51.4	5.2	37819.9	362.4	metabolic process; transport	1.45
A0A1P8D6J8	Phycobilisome rod-core linker polypeptide	42	8	89	2	228	26.6	9.04	15136.3	53.5	metabolic process	1.17
P54270	Glyceraldehyde-3-phosphate dehydrogenase, cytosolic	73	20	293	20	335	36.1	6.25	44867.2	405.6	metabolic process	0.90
A0A1P8D6G7	ATP synthase subunit alpha	24	10	79	4	503	54.5	5.03	9638.5	92.4	metabolic process; transport	0.60
A0A1C9CEX0	Phycobilisome rod-core linker protein	22	4	45	1	235	27.4	8.03	4532.7	45.8	metabolic process	0.59
W8DW78	Allophycocyanin gamma subunit	35	3	51	3	161	18.2	5.36	9925.5	94.2	metabolic process;	0.49

											transport	
D7USG8	Elongation factor like (Fragment)	40	7	82	7	246	27.4	9	9860.7	102.0	metabolic process	0.42
A0A141SEG3	Thiol-specific antioxidant protein	10	2	18	2	199	22.4	4.93	3306.8	38.6	cellular homeostasis; metabolic process; regulation of biological process	0.24
A0A1P8D6I7	Putative rubisco expression protein	51	12	54	5	290	32.9	6.19	7493.1	69.8		0.21
A0A1P8D6K4	Allophycocyanin beta-18 subunit	22	4	26	4	169	19.5	5.08	4116.9	45.7	metabolic process; transport	0.19
Q6B8V2	Chaperone protein dnaK	16	5	22	5	621	68	5.08	4762.3	49.9	cell organization and biogenesis; metabolic process	0.14
A0A141SES2	Photosystem II protein D1	8	2	5	2	360	39.6	5.67	755.8	7.7	metabolic process; response to stimulus; transport	0.10
Q9ZSL9	UTP--glucose-1-phosphate uridylyltransferase	26	7	24	7	495	55	6.76	4206.6	48.1	metabolic process	0.09
R4NRR5	GDP-mannose-3', 5'-epimerase	23	5	32	5	350	38.9	6.09	4271.9	34.3	metabolic process	0.09
W8DVZ1	Elongation factor Tu, chloroplastic	39	9	41	9	409	44.7	5.1	6005.8	55.9	metabolic process	0.08
A0A1C9CEU3	Ribosomal protein S4	8	2	10	2	201	23	10.08	1870.9	15.9	metabolic process	0.04
A0A1C9CF93	Photosystem II CP47 reaction center protein	19	8	30	8	509	56.3	6.9	4820.1	54.6	metabolic process	0.03
A0A141SEU1	60 kDa chaperonin	15	4	13	2	528	57	5.95	1304.6	17.5	metabolic process	0.03
A0A1C9CET5	Phycobilisome core-membrane linker protein	2	2	20	2	887	101.2	9.38	1895.0	6.6	metabolic process	0.03
O48511	Galactose-1-phosphate uridylyltransferase	11	3	8	3	369	42.4	6.57	1480.5	14.7	metabolic process	0.02
P48492	Triosephosphate isomerase, cytosolic (Fragment)	16	2	6	2	250	26.7	5	962.7	8.2	metabolic process	0.02
A0FLC3	Elongation factor 2 (Fragment)	6	2	4	2	561	62.6	6.04	376.4	3.3	metabolic process	0.01

W8DWE8	Thioredoxin	34	2	3	2	110	12.2	5.85	593.4	3.6	cellular homeostasis; metabolic process; regulation of biological process	0.01

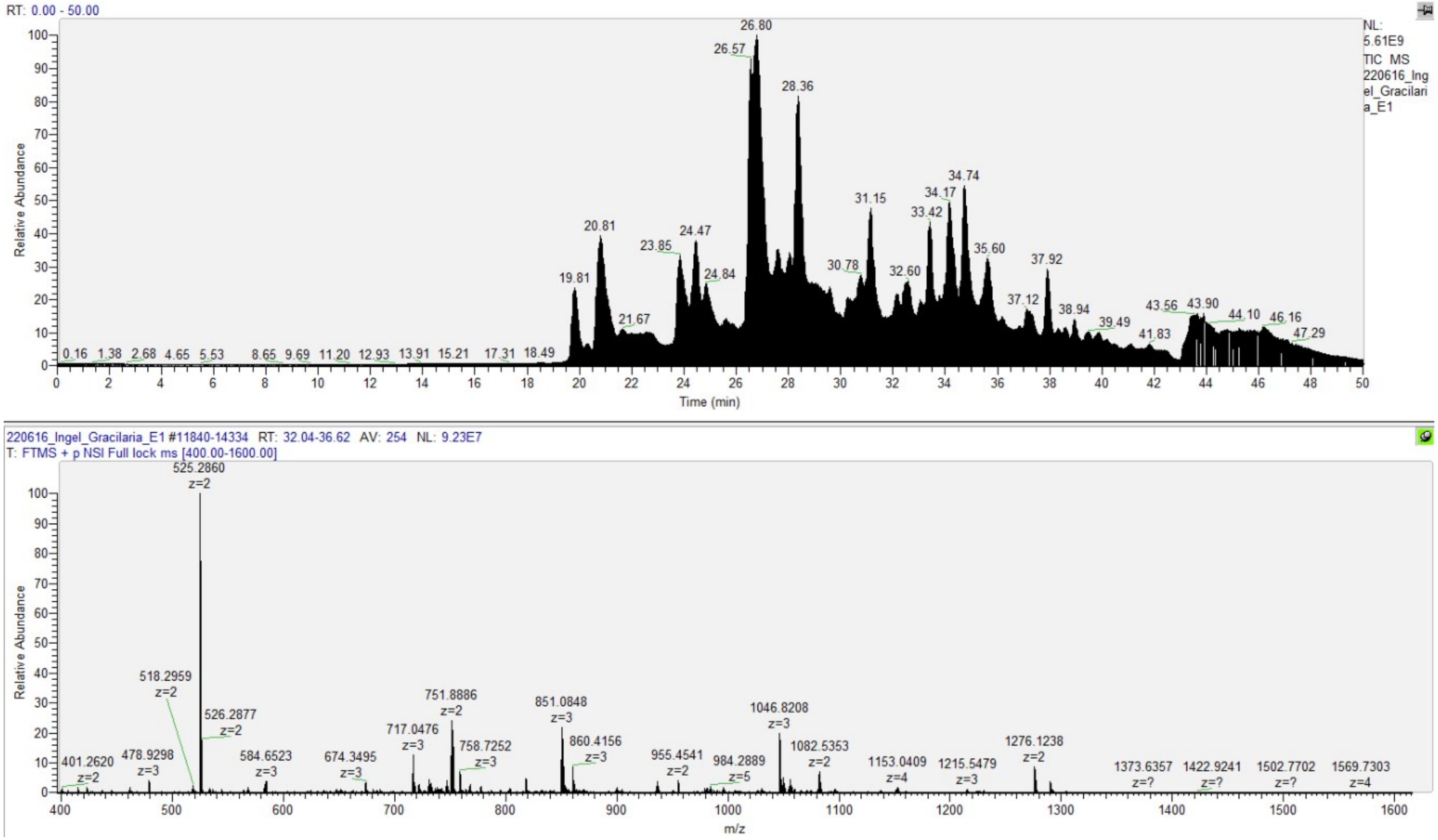

Fig. S1. Representative nanoHPLC chromatogram of the injection of the tryptic digest of a SDS-PAGE spot (panel A), and a representative mass spectrum acquired during the run (panel B).

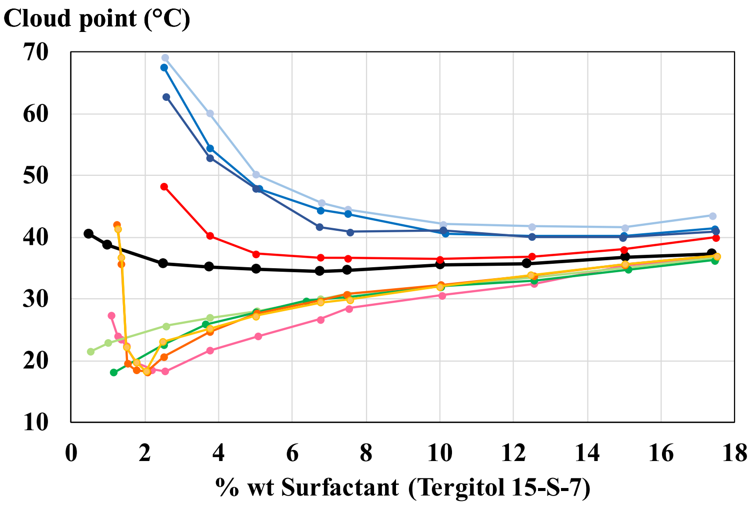

Fig. S2. Binodal curves of Tergitol 15-7-7 with 0.3 wt% of SAILs, at pH 7.0: ●, Tergitol 15-S-7 neat system; ●, [$P_{6,6,6,14}$]Cl; ●, [$P_{6,6,6,14}$]Br; ●, [$P_{6,6,6,14}$][Dec]; ●, [$P_{6,6,6,14}$][TMPP]; ●, [$P_{4,4,4,14}$]Cl; ●, [$P_{8,8,8,8}$]Br; ●, [C_{10}mim]Cl; ●, [C_{12}mim]Cl; and ●, [C_{14}mim]Cl. Maximum deviation error is 1ºC.

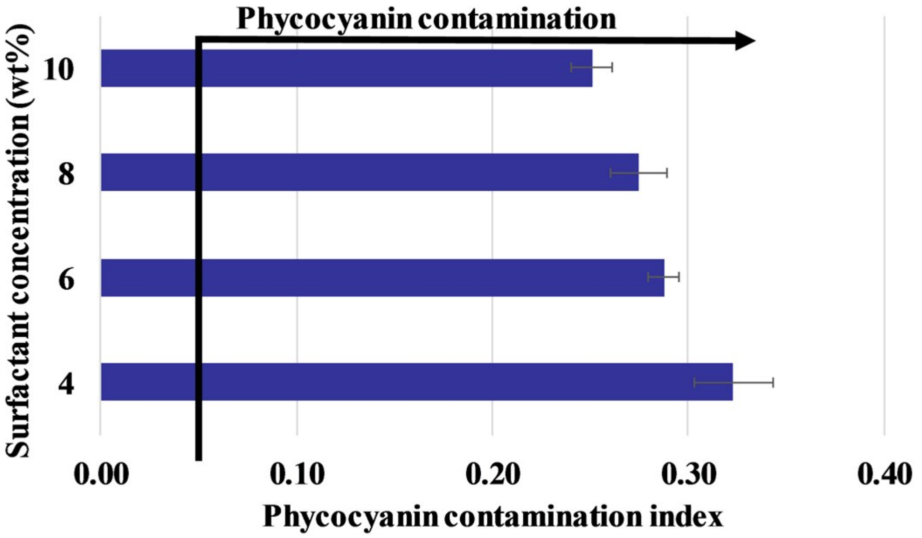

Fig. S3. Surfactant concentration effect upon the R-phycoerythrin contamination with R-phycocyanin.

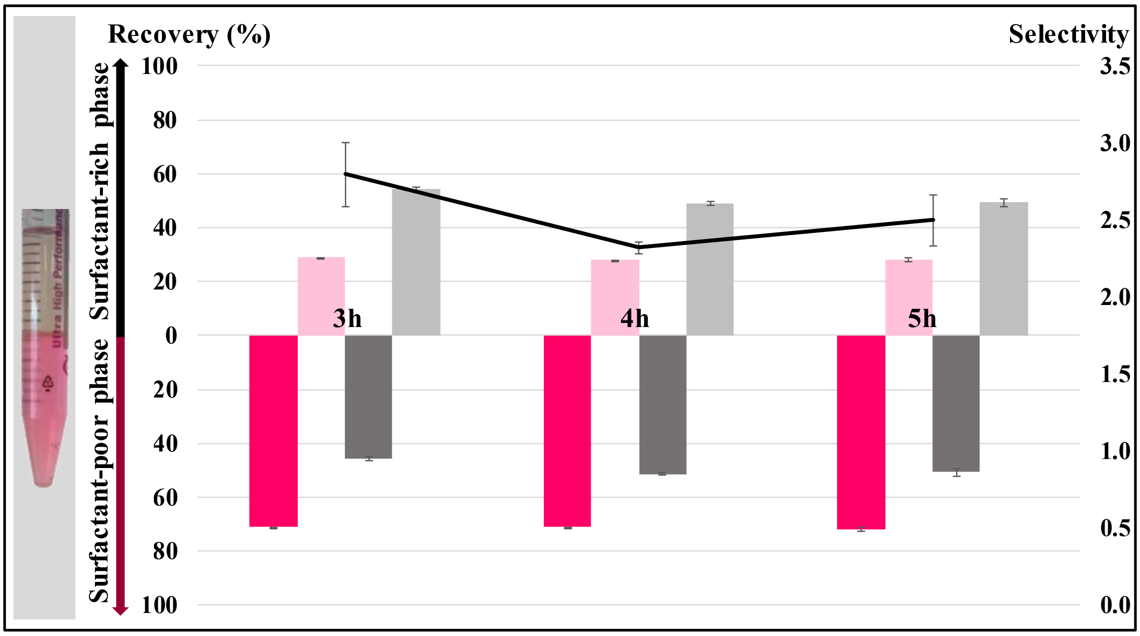

Fig. S4. Extraction time effect upon the recovery of R-phycoerythrin and total proteins towards the surfactant-rich and -poor phases: 🟥 and □, R-phycoerythrin recovery (%) in the surfactant-poor and surfactant-rich phases, respectively; ■ and ▨, total proteins recovery (%) in the surfactant-poor and surfactant-rich phases, respectively. The line represents the selectivity.

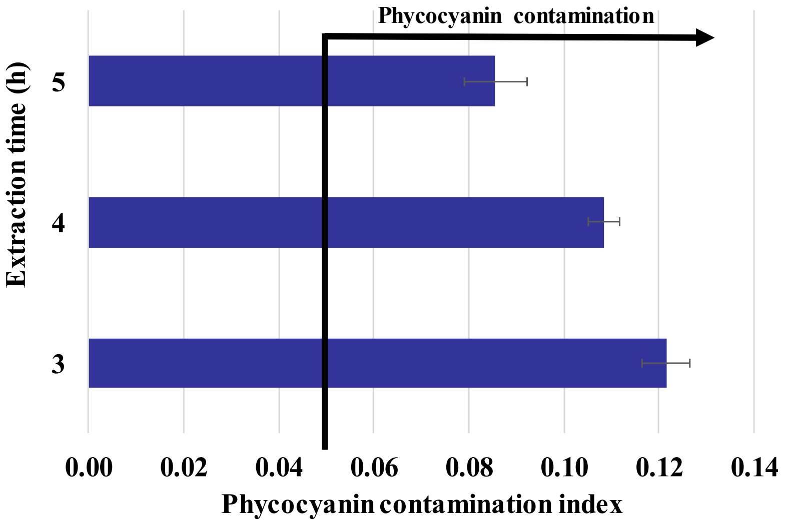

Fig. S5. Extraction time effect upon the R-phycoerythrin contamination with R-phycocyanin.

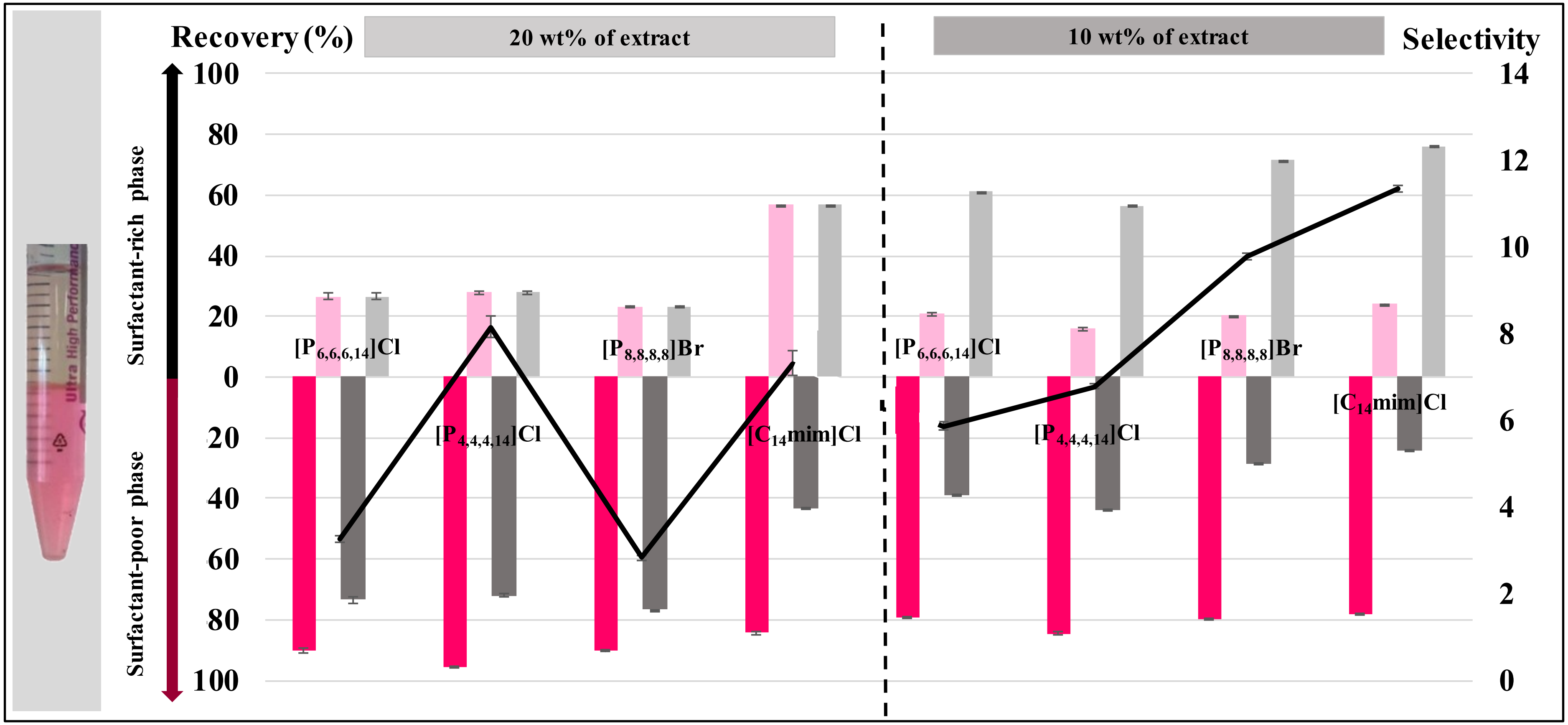

Fig. S6. Phycobiliproteins extract concentration influence on the recovery of R-phycoerythrin and total proteins towards the surfactant-rich and -poor phases: ■ and □, R-phycoerythrin recovery (%) in the surfactant-poor and surfactant-rich phases, respectively; ■ and □, total proteins recovery (%) in the surfactant-poor and surfactant-rich phases, respectively. The line represents the selectivity.

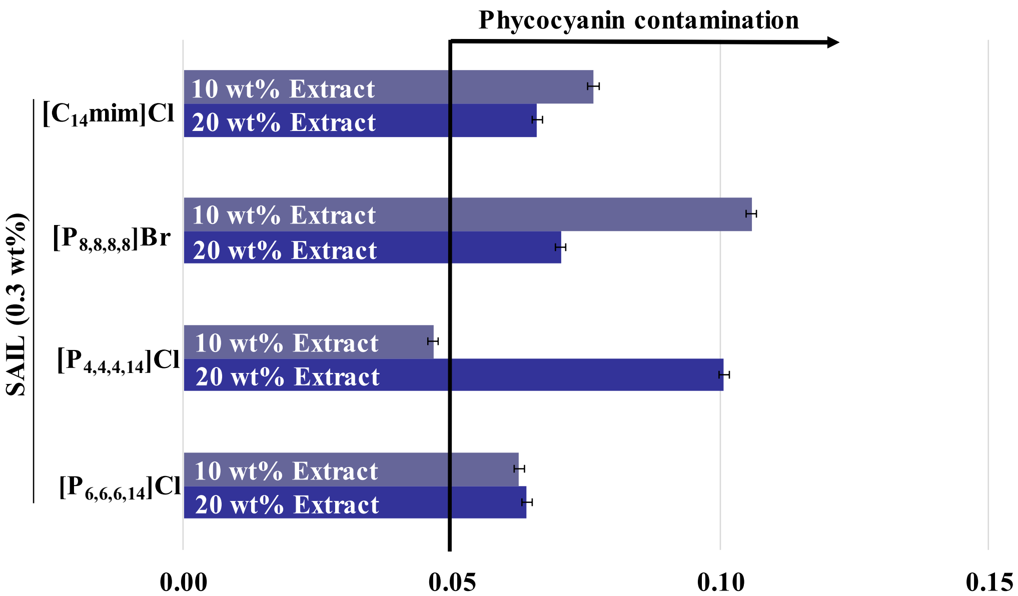

Fig. S7. Phycobiliproteins extract concentration influence on the R-phycoerythrin contamination with R-phycocyanin.

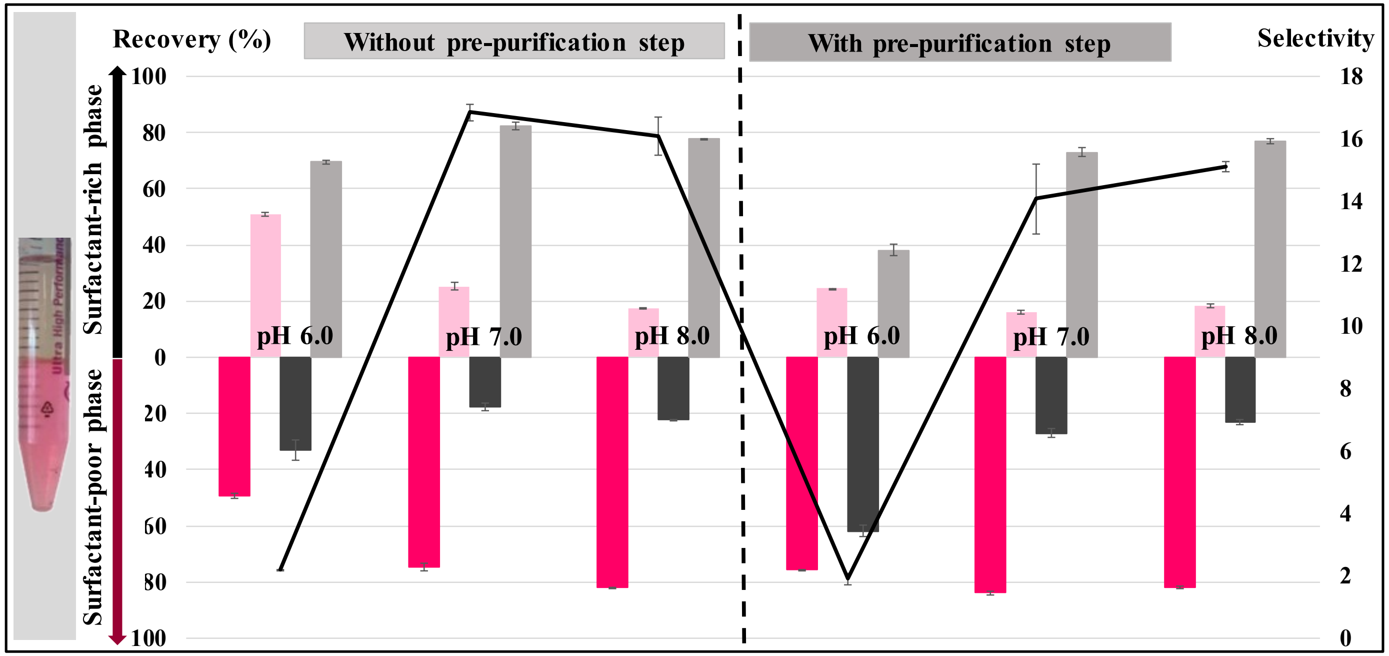

Fig. S8. Effects of the system pH as well as a pre-purification step before the liquid-liquid extraction upon the recovery of R-phycoerythrin and total proteins towards the surfactant-rich and -poor phases: ■ and □, R-phycoerythrin recovery (%) in the surfactant-poor and surfactant-rich phases, respectively; ■ and □, total proteins recovery (%) in the surfactant-poor and surfactant-rich phases, respectively. The line represents the selectivity.

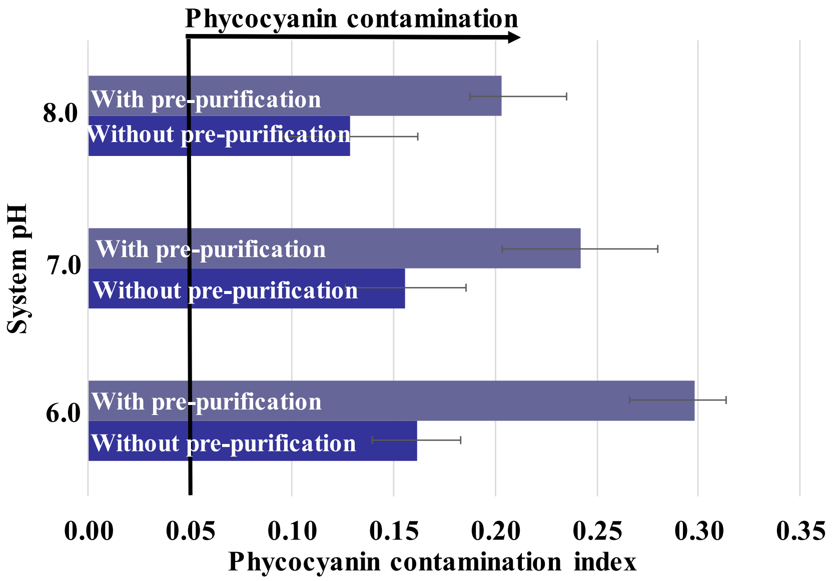

Fig. S9. Effects of the system pH as well as a pre-purification step before the liquid-liquid extraction upon the R-phycoerythrin contamination with R-phycocyanin.

Phase formers recycling

ATR-FTIR measurements were carried out to evaluate the possible separation of surfactant and SAIL from the surfactant-rich phase. Briefly, 4 mL of cold acetone was added to 1 mL of the surfactant-rich phase of the mixed AMTPS composed of Tergitol 15-S-7 and $[N_{1,1,12,(C7H7)}]Br$ to disrupt the micelles and, consequently, to precipitate the proteins inside. The tube was left for 1 h at -20°C and then centrifuged for 30 min at 4°C and 5000 rpm. As a result, a proteinic pellet and an acetone supernatant were obtained. The pellet was resuspended in 1 mL of water, and both the resuspended pellet and the acetone supernatant were analyzed using FTIR system Spectrum BX, PerkinElmer, equipped with a single horizontal Golden Gate ATR cell, and a diamond crystal. All data were recorded at room temperature, in the range of 4000 – 500 cm^{-1} by accumulating 32 scans with a 4 cm^{-1} and a 2 cm^{-1} interval. Two replicas of each sample were analysed, and their average considered and normalized. These results are shown in Fig. S9.

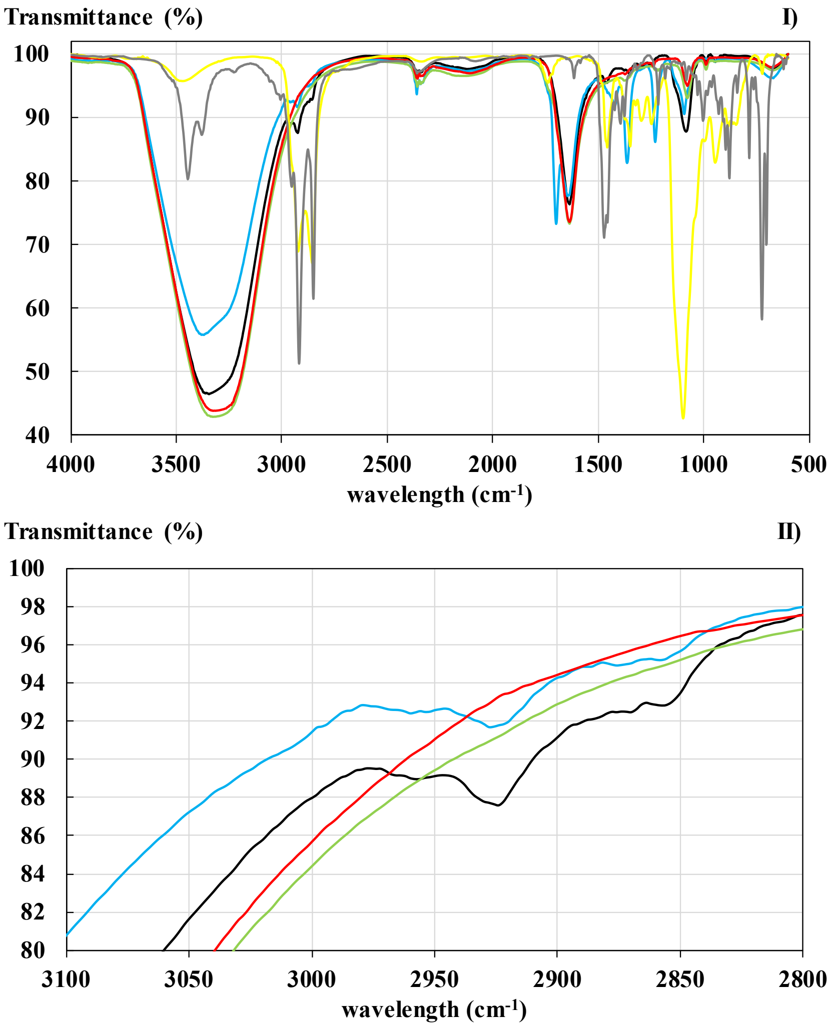

Fig. S10. FTIR analysis of Tergitol 15-S-7 (—), $[\mathrm{N}_{1,1,12,(\mathrm{C7H7})}]$Br (—), both phases of the mixed AMTPS composed of 10 wt% of Tergitol 15-S-7 + 0.3 wt% of $[\mathrm{N}_{1,1,12,(\mathrm{C7H7})}]$Br + 89.7 wt% of McIlvaine buffer pH 7.0 as the blank control: (—), surfactant-poor phase and (—), surfactant-rich phase; and the surfactant-rich phase of an identical AMTPS but with 10 wt% of phycobiliproteins extract after being precipitated with cold acetone, resulting in an acetone supernatant and a pellet resuspended in water: (—), acetone supernatant and (—), pellet resuspended in water.